Published in final edited form as:

Pediatr Radiol. 2015 April ; 45(4): 593–605. doi:10.1007/s00247-014-3210-y.

Common normal variants of pediatric vertebral development that mimic fractures: a pictorial review from a national longitudinal bone health study

Jacob Lester Jaremko, MD, PhD[1,*], **Kerry Siminoski, MD**[2], **Gregory Firth, MMed**[3], **Mary Ann Matzinger, MD**[4], **Nazih Shenouda, MD**[4], **Victor N. Konji, PhD**[5], **Johannes Roth, MD**[6], **Anne Marie Sbrocchi, MD**[7], **Martin Reed, MD**[8], **Kathleen O'Brien, MD**[9], **Helen Nadel, MD**[10], **Scott McKillop, MD**[11], **Reinhard Kloiber, MD**[12], **Josée Dubois, MD**[13], **Craig Coblentz, MD**[14], **Martin Charron, MD**[15], **Leanne M. Ward, MD**[6], and **the Canadian STOPP Consortium**[16]

[1]Department of Radiology & Diagnostic Imaging, University of Alberta, Edmonton, Canada

[2]Department of Radiology and Diagnostic Imaging and Department of Medicine, University of Alberta, Edmonton, Canada

[3]Paediatric Orthopaedic Unit, Chris Hani Baragwanath Academic Hospital, Johannesburg South Africa

[4]Department of Diagnostic Imaging, University of Ottawa, Ottawa, Canada

[5]Pediatric Bone Health Clinical Research Program, Children's Hospital of Eastern Ontario, Ottawa, Canada

[6]Department of Pediatrics, University of Ottawa, Ottawa, Canada

[7]Department of Pediatrics, McGill University, Montreal, Canada

[8]Department of Radiology, University of Manitoba, Winnipeg, Canada

[9]Department Diagnostic Imaging, Dalhousie University, Halifax, Canada

[10]Department of Radiology, University of British Columbia, Vancouver, Canada

[11]Department of Radiology, University of Western Ontario, London, Canada

[12]Department of Radiology, University of Calgary, Calgary, Canada

[13]Department of Radiology, Universite de Montreal, Montreal, Canada

[14]Department of Radiology, McMaster University, Hamilton, Canada

[15]Department of Radiology, University of Toronto, Toronto, Canada

[16]National Pediatric Bone Health Working Group

Abstract

[*]Corresponding author: Jacob Lester Jaremko, MD, PhD, Department of Radiology and Diagnostic Imaging, 2A2.41 WC Mackenzie Health Sciences Centre, University of Alberta, 8440-112 Street, Edmonton, Alberta T6G 2B7, Tel: (780) 407-6907, Fax: (780) 407-3853, jjaremko@ualberta.ca.

Conflicts of Interest: None.

Children with glucocorticoid-treated illnesses are at risk for osteoporotic vertebral fractures and growing awareness has led to increased monitoring for these fractures. However scant literature describes developmental changes in vertebral morphology that can mimic fractures. The goal of this paper is to aid in distinguishing between normal variants and fractures. We illustrate differences using lateral spine radiographs obtained annually from children recruited to the Canada-wide **ST**eroid-Associated **O**steoporosis in the **P**ediatric **P**opulation (STOPP) observational study, in which 400 children with glucocorticoid-treated leukemia, rheumatic disorders, and nephrotic syndrome were enrolled near glucocorticoid initiation and followed prospectively for 6 years.

Normal variants mimicking fractures exist in all regions of the spine and fall into two groups. The first group comprises variants mimicking pathological vertebral height loss, including not-yet-ossified vertebral apophyses superiorly and inferiorly which can lead to a vertebral shape easily over-interpreted as anterior wedge fracture, physiologic beaking, and spondylolisthesis associated with shortened posterior vertebral height. The second group includes variants mimicking other radiologic signs of fractures: anterior vertebral artery groove resembling an anterior buckle fracture, Cupid's bow balloon disk morphology, Schmorl nodes mimicking concave endplate fractures, and parallax artifact resembling endplate interruption or biconcavity.

If an unexpected vertebral body contour is detected, careful attention to its location, detailed morphology, and (if available) serial changes over time may clarify whether it is a fracture requiring change in management or simply a normal variant. Awareness of the variants described in this paper can improve accuracy in the diagnosis of pediatric vertebral fractures.

Keywords

Osteoporosis; Normal variants; Spine; Fracture; Radiography; Child

Introduction

Vertebral compression fractures occur in children in the setting of accidental or non-accidental trauma [1], or osteoporosis which can be primary or secondary. Secondary osteoporosis is seen with chronic disease and/or glucocorticoid use [2–7]. Accurate diagnosis of compression fractures is particularly difficult in children because of the normal variants and changes associated with normal vertebral development, some of which can mimic fractures. The purpose of this report is to demonstrate these morphological variants and to provide a practical guide to differentiating thoracic and lumbar fractures from normal variants in children at different ages and stages of development.

Materials and methods

Most of the radiographs in this study were acquired through **ST**eroid-associated **O**steoporosis in the **P**ediatric **P**opulation (**STOPP**) research program, a pan-Canadian multi-center longitudinal observational study funded by the Canadian Institutes for Health Research. In this study, 404 children were enrolled about the time of glucocorticoid initiation, at a median age of 6.2 years, range 1–17 years; 50% boys; 188 (46%) had

leukemia, 136 (34%) rheumatic conditions, and 80 (20%) nephrotic syndrome. The study was approved by the Ethics Board at each institution and informed consent/assent was obtained, as appropriate. As one of the key components of the STOPP study, the children underwent lateral thoracolumbar spine radiographs at baseline and annually up to 6 years following glucocorticoid initiation to document the frequency and pattern of baseline and incident vertebral fractures. Full descriptions of this cohort and the prevalence and incidence of vertebral fractures as well as associated risk factors have been published elsewhere [2–8]. The annual radiographs from patients enrolled in the STOPP study demonstrate a wide range of vertebral fractures and normal variants, providing source material for this pictorial review in partial fulfilment of the original objectives of the STOPP study. To illustrate some findings not observed in the STOPP films, we used anonymized radiographs from other patients obtained during routine clinical practice.

Normal ossification

Vertebrae begin developing as condensations of mesenchymal cells around the notochord, whose remnants form the intervertebral disks [9]. Normal vertebrae form by coalescence of primary ossification centers in the prenatal period, and then by fusion of the posterior neural arch with the vertebral body in the first 3 to 6 years of life. There are thought to be three primary and five secondary ossification centres [9]. The endplates represent zones of provisional calcification at originally cartilaginous growth plates [10]. Ossification is complex and varies by spinal level, with little apparent relation between anterior and posterior elements [11]. Cervical vertebrae have some unique developmental features and are not considered in this review. In later childhood and early puberty, secondary ossification centers (apophyses) develop at tips of spinous and transverse processes, and they also encircle the margins of the superior and inferior endplates (known as ring apophyses) [9] [FIGURE 1]. These do not completely fuse until adulthood. The ring apophyses are true apophyses in that they do not contribute to vertebral growth [12]. Sharpey’s fibres of the disc annulus attach to this, a zone involved in annular tears [13] and syndesmophytes in spondyloarthropathy [14].

The shape of each vertebra and the overall kyphotic and lordotic curves of the spinal column evolve throughout a child’s development [15]. Analysis of vertebral contour on radiographs should consider the shape of adjacent vertebrae, alignment with respect to other vertebrae, changes in serial radiographs, and appearance relative to other children of similar age.

Defining a vertebral fracture

A fracture implies that bony integrity is compromised. An interruption of the endplate or cortex is, therefore, the most direct sign of fracture [16], but is not always visible on radiographs because of factors such as the angle of projection or incomplete vertebral ossification. Because the spine is routinely under compressive load, many vertebral fractures develop loss of height from lost endplate integrity at some part of the vertebral body. Therefore, on radiographs a vertebral fracture will usually appear as either a site of endplate interruption, height loss, or both. However, distinguishing between normal variation and fracture is often difficult. Normal variants should be asymptomatic, but the absence of pain or tenderness does not exclude fractures, which are also frequently asymptomatic in adults

[17] and in children with glucocorticoid-treated illnesses [2–5, 7]. On serial radiographs, deformities can disappear over time, whether due to normal variation or fracture. This is because children have the capacity to reshape previously fractured vertebral bodies through bone modeling, restoring normal vertebral dimensions through endochondral bone formation if there is sufficient residual linear growth in the spine [18–20].

For individual patients, additional imaging such as bone scan, MRI, or CT scan can support the diagnosis of a fracture by detecting findings such as active bone remodeling, marrow edema, or subtle fracture lines, respectively [1]. However, each of these modalities has its own pitfalls: limited spatial resolution at bone scan, limited evaluation of the proton-poor cortex at MRI, and high radiation dose at CT scan. CT scans also require sagittal reformations for optimal sensitivity [21]. It is still desirable to be as specific as possible regarding presence of a fracture based on radiographic appearance. Evidence-based morphologic rules can be of value in this setting. Serial evaluations of spine morphometry are particularly important to most accurately determine the presence of pathology in at-risk patients, because, incident changes in vertebral height and wedging are likely to be fractures [22].

Endplate parallelism and fracture

By adulthood, vertebral bodies are in general rectangular structures with parallel endplates. Loss of endplate parallelism is a key sign of vertebral fracture. In adults and children both, semi-quantitative scoring systems are used to determine whether lost height and parallelism are sufficient to diagnose a fracture [17]. In the Genant semi-quantitative (GSQ) grading system [23, 24], wedge fractures show anterior height loss, so-called biconcave fractures have central depression (but despite the name, often only involve one endplate), while those referred to as crush fractures show posterior depression. Severity of any of these fracture types is classified based on the percentage of height loss [FIGURE 2, FIGURE 3]. Since L5 has unique shape features it is not scored in the GSQ system. An alternative semi-quantitative scoring system is the Algorithm-Based Qualititative (ABQ) approach [22], in which evidence of endplate disruption is the primary sign of fracture. In ABQ assessment of adult spines for osteoporotic fractures, the observer asks sequentially (1) Is the apparent depression of the endplate close to its center? Is it not a result of oblique projection? and (3) Does it involve the entire endplate; if all answers are yes then a fracture is probable [22]. The ABQ approach, particularly considering loss of endplate parallelism, endplate depression and anterior cortical buckling as signs of fracture, has also been applied to pediatric vertebral fracture evaluation, but only to a limited degree [2].

In all of the above situations, endplates are no longer parallel, at least focally. However, endplates in children are not usually parallel to each other. Vertebrae in normal young children typically appear convex outwards, as if the bone were bulging, because of incomplete ossification of the periphery, with a gradual transition to a more adult shape with slightly concave endplates [FIGURE 4]. This limits the application of the ABQ approach in the pediatric population.

A. Findings mimicking anterior wedge compression fracture

Anterior wedging: physiologic thoracolumbar wedging vs. compression fracture

Normal thoracic kyphosis and lumbar lordosis develop progressively from early childhood to adulthood [25]. Likely to accommodate the spinal transition from kyphosis to lordosis, there is often mild physiologic vertebral wedging, subjectively most prominent in mid thoracic spine although we are not aware of peer-reviewed studies quantifying this in children. The degree of wedging near the thoracolumbar junction, from T10-L3, has been studied in more detail, with 95% of children of any age having less than 11% anterior height loss in this region [26]. Wedging greater than this is suspicious for a fracture. However, the acceptable limit of wedging in the upper thoracic spine or lumbar spine has not been comprehensively studied in children. Because of the wide range of normal variation, the widely used Genant scoring system allows a relatively generous 20% height loss as the minimum threshold to define a wedge fracture [23, 24]. There is clearly some developmental variation in relative vertebral body heights, which likely also accounts for the finding in adults that short vertebral height (SVH) alone without other markers of fracture is unrelated to osteoporosis [27]. Loss of normal outward convexity of the endplates posteriorly also suggests a fracture, although preservation of this convexity does not exclude a fracture [FIGURE 5]. Diagnosis of a mild anterior wedge compression fracture can be difficult, but has important prognostic significance. For example, in the STOPP study, the presence of Genant grade 1 fracture (20–25% height loss) at baseline in children with leukemia was independently associated with an increased risk of new fractures in the first 12 months following chemotherapy initiation [3].

Anterior wedging: ring apophyses

Before the ring apophyses ossify there is a small radiolucent defect at anterior endplates, that can at times form a prominent irregular notch. This type of endplate interruption is physiologic and not a fracture. We have noted that preserved outward convexity of the endplate immediately posterior to this is a clue that this is a normal variant, because a fracture would be unlikely to involve the strong anterior cortex and not also involve the relatively weak unsupported endplate directly posterior to it [FIGURE 6].

Anterior cortical buckling vs. vertebral artery impression

The anterior vertebral artery impression is a thin, transverse linear indentation in anterior cortex, usually with adjacent convexity above and below. On careful inspection this can be differentiated from a fracture, which would generally be associated with anterior wedging. [FIGURE 7]

Anterior cortical buckling: beaking in dysplasia or neuromuscular disease

Accentuation of normal physiological anterior vertebral body beaking at the thoracolumbar junction is seen in conditions affecting epiphyses or epiphyseal equivalents such as the ring apophyses. These include neuromuscular disease, skeletal dysplasias such as the mucopolysaccharidoses, and congenital hypothyroidism [28] and may be associated with gibbus deformity when severe [29]. This finding, possibly related to anterior disk herniation

under abnormal loading [28], should not be confused with wedge compression fracture. In each of the mucopolysaccharidoses, the beaking resembles a prominent impression at an un-ossified ring apophysis [FIGURE 8].

B. Findings mimicking central endplate fractures

Smooth undulating endplate: Cupid's bow/balloon disk

Cupid's bow refers to a smooth concavity centered at the posterior third of the endplate, usually the inferior endplate at L3, L4 and L5 [30], and is rarely seen in the thoracic spine. This is a recognized vertebral variant seen throughout life. The cortex of the concavity is intact and the finding typically becomes less marked in successive vertebrae moving caudally. A very similar variant is balloon disk, observed when both adjacent endplates have similar bowing [31].

The reference to Cupid's bow may be most obvious based on antero-posterior (AP) image, on which the bowing is seen as adjacent left and right parasagittal superior indentations. In cadaveric studies the depressed or indented areas of endplates are sites of focally absent cartilage, likely associated with reduced vertebral growth in these areas during spinal development [32]. Cupid's bow deformity is not associated with decreased bone density or other pathologic conditions [32]. Balloon disk was seen in 15% of 612 Japanese teenagers and also had no association with pain or pathologic conditions [31]. A concave inferior endplate fracture can closely mimic Cupid's bow or balloon disk, but on close inspection a fracture would be expected to have endplate interruption and have indentation centered more anteriorly, without symmetrical involvement of adjacent vertebrae [FIGURE 9].

Non-overlapping endplates: parallax

Because radiographs are obtained with the image source located at a finite distance from the film, vertebrae far from the central ray may have parallel but non-overlapping endplates, giving a bone-in-bone appearance where the side of the vertebra farther from the source is less magnified than the other side. This can produce confusing images mimicking fracture, particularly of the biconcave type. Close inspection of adjacent vertebrae for the expected similar effects, and if necessary a repeat film obtained with the central ray closer to the vertebra in question, should distinguish this artifact from endplate interruption associated with fracture. [FIGURE 10]

Focally interrupted endplate: Schmorl node

Focal endplate interruption is frequently due to intraosseous herniation of the intervertebral disk, known as a Schmorl node [10]. These nodes are most common in the lower thoracic to upper lumbar spine. Most, are asymptomatic [33]. Many potential causes have been identified, from developmental variation to axial loading trauma (e.g., gymnasts) and disk or endplate degeneration [33]. It is likely that Schmorl nodes occur for any reason that causes disk nuclear pressure to be greater than the failure stress of the adjacent endplate. A developmental gap or focal thinning in endplate cortex could lead to this, with little clinical significance, or an osteoporotic endplate could develop Schmorl nodes as part of a compression fracture. The significance of these nodes thus may depend on adjacent findings.

The distinction between a Schmorl node (effectively a small focal endplate fracture) from other fractures thought to have greater clinical significance rests on detecting overall vertebral height loss or endplate depression. [FIGURE 11 (a)] In our experience, Schmorl nodes often are outlined by sclerosis.

Diffusely irregular endplates: Scheuermann disease

The full expression of Scheuermann disease includes anterior thoracic or thoracolumbar vertebral wedging, irregular endplates containing multiple Schmorl nodes [10], early disk degeneration, and clinically progressive thoracic hyperkyphosis and back pain [34, 35]. It is diagnosed radiographically by kyphosis >45° in neutral standing position, with wedging of 3 or more adjacent vertebrae by more than 5° each [34]. Onset of wedging is often just after ossification of ring apophyses begin, related to decreased anterior vertebral height growth [35]. The underlying cause of Scheuermann disease is unclear and may relate to a combination of genetic and mechanical factors impairing normal development of anterior cortex, disk and endplates. A study of medieval cadaver spines suggested Scheuermann disease could be be a result of so called subadult Schmorl nodes occurring before spinal maturity [36]. The endplate irregularity and anterior wedging of Scheuermann disease can mimic multiple compression fractures. Endplates have more diffuse and more prominent irregularity in Scheuermann kyphosis than in most fractures. [FIGURE 11(b)]

Multilevel biconcave endplates: Sickle cell anemia

Children with sickle cell anemia develop a characteristic vertebral body deformity described as “H-shaped,” “Lincoln log,” or “fish-mouth” with biconcave central endplate depression often having relatively abrupt anterior and posterior margins [37] [FIGURE 12]. Contributing to bone softening, these children have decreased bone mineral density [38] and are susceptible to marrow infarction [37]. It is unclear whether the endplate depressions occur as a result of clinically silent fractures, as a more chronic modeling process, or by both mechanisms. In any patient with multi-level biconcave endplate depression, the possibility of sickle cell anemia should be considered.

C. Findings mimicking posterior fractures

Trapezoidal L5 shape (short posterior vertebral body wall)

Because the L5 vertebra has different shape from other thoracic and lumbar vertebrae, it is not included in the GSQ fracture grading system [23]. A short posterior vertebral body wall at a trapezoidal L5 is unlikely to represent a posterior crush fracture as it might at other levels, because it is frequent a normal variant [FIGURE 13]. There is a possible association of this finding with spondylolysis, although studies on this topic have been contradictory [39–41]. Because spondylolysis may be clinically significant for the patient, finding a short L5 posterior body wall should prompt the radiologist to carefully assess for a pars defect.

Incomplete midline fusion

A sagittal fissure indicating incomplete midline fusion of posterior element ossification centers, sometimes termed spina bifida occulta, is not usually mistaken for a fracture, but occasionally these fissures can be eccentric or oblique, causing diagnostic uncertainty

[FIGURE 14]. Sclerosis and smooth appearance of fissure margins suggests a developmental variant. Other rare segmentation anomalies such as butterfly vertebrae or dorsal hemivertebra can also mimic fractures [42], especially if only a lateral radiograph is reviewed.

Summary

A variety of normal variants, some unique to children, mimic each of the types of vertebral compression fractures [TABLE 1]. Careful attention to the location, detailed morphology, and time of onset and progression (if known) of a questionable finding can clarify whether it is a fracture or normal variant. Diagnosis of a vertebral compression fracture in a child is best made by experienced observers combining quantitative methods such as Genant grading with the qualitative features discussed in this study. A correct diagnosis has significant clinical consequences, because vertebral fractures in the absence of high-force trauma may indicate bone fragility, leading to recommendations for bone-specific treatment (such as osteoporosis medications) or modification of therapy targeting the underlying disease (such as glucocorticoid dose).

Acknowledgments

This study was primarily funded by an operating grant from the Canadian Institutes for Health Research (FRN 64285). Additional funding for this work has been provided to Dr. Leanne Ward by the Canadian Institutes for Health Research New Investigator Program, the Canadian Child Health Clinician Scientist Career Enhancement Program, a University of Ottawa Research Chair Award and the CHEO Departments of Pediatrics and Surgery. This work was also supported by the Children's Hospital of Eastern Ontario Research Institute and the University of Alberta Women and Children's Health Research Institute.

The Canadian STOPP Consortium would like to thank the following individuals:

The children and their families who participated in the study and without whom the STOPP study would not have been possible.

Research Associates who managed the study at the co-ordinating center (the Children's Hospital of Eastern Ontario Ottawa, Ontario): Elizabeth Sykes (STOPP Project Manager), Maya Scharke (STOPP Data Analyst and Database Manager), Monica Tomiak (Statistical Analyses), Victor Konji (STOPP Publications and Presentations Committee Liaison), Steve Anderson (Children's Hospital of Eastern Ontario Pediatric Bone Health Program Research Manager), Catherine Riddell (STOPP National Study Monitor);

Research Associates who took care of the patients from the following institutions: Alberta Children's Hospital, Calgary, Alberta: Eileen Pyra; British Columbia Children's Hospital, Vancouver British Columbia: Terry Viczko, Sandy Hwang, Angelyne Sarmiento; Children's Hospital of Eastern Ontario, Ottawa, Ontario: Heather Cosgrove, Josie MacLennan, Catherine Riddell; Children's Hospital, London Health Sciences Centre, London, Ontario: Vinolia ArthurHayward, Leila MacBean, Mala Ramu; McMaster Children's Hospital, Hamilton, Ontario: Susan Docherty-Skippen; IWK Health Center, Halifax, Nova Scotia: Cindy Campbell, Aleasha Warner; Montréal Children's Hospital, Montréal, Québec: Valérie Gagné, Diane Laforte, Maritza Laprise; Ste. Justine Hospital, Montréal, Québec: Claude Belleville, Natacha Gaulin Marion; Stollery Children's Hospital, Edmonton, Alberta: Ronda Blasco, Germaine McInnes; Amanda Mullins; Toronto Hospital for Sick Children, Toronto, Ontario: Alexandra Airhart, Michele Petrovic, Nicole Sarvaria; Winnipeg Children's Hospital, Winnipeg, Manitoba: Dan Catte, Erika Bloomfield, Jeannine Schellenberg. The Research Nurses, Support Staff and all the STOPP collaborators from the various Divisions of Nephrology, Oncology, Rheumatology and Radiology who have contributed to the care of the children enrolled in the study.

References

1. Leroux J, Vivier PH, Ould Slimane M, Foulongne E, Abu-Amara S, Lechevallier J, Griffet J. Early diagnosis of thoracolumbar spine fractures in children. A prospective study. Orthop Traumatol Surg Res. 2013; 99:60–65. [PubMed: 23276683]

2. Halton J, Gaboury I, Grant R, et al. Advanced vertebral fracture among newly diagnosed children with acute lymphoblastic leukemia: results of the Canadian Steroid-Associated Osteoporosis in the Pediatric Population (STOPP) research program. J Bone Miner Res. 2009; 24:1326–1334. [PubMed: 19210218]
3. Alos N, Grant RM, Ramsay T, et al. High incidence of vertebral fractures in children with acute lymphoblastic leukemia 12 months after the initiation of therapy. J Clin Oncol. 2012; 30:2760–2767. [PubMed: 22734031]
4. Huber AM, Gaboury I, Cabral DA, et al. Prevalent vertebral fractures among children initiating glucocorticoid therapy for the treatment of rheumatic disorders. Arthritis Care Res (Hoboken). 2010; 62:516–526. [PubMed: 20391507]
5. Rodd C, Lang B, Ramsay T, et al. Incident vertebral fractures among children with rheumatic disorders 12 months after glucocorticoid initiation: a national observational study. Arthritis Care Res (Hoboken). 2012; 64:122–131. [PubMed: 22213727]
6. Feber J, Gaboury I, Ni A, et al. Skeletal findings in children recently initiating glucocorticoids for the treatment of nephrotic syndrome. Osteoporos Int. 2012; 23:751–760. [PubMed: 21494860]
7. Phan V, Blydt-Hansen T, Feber J, et al. Skeletal findings in the first 12 months following initiation of glucocorticoid therapy for pediatric nephrotic syndrome. Osteoporos Int. 2014; 25:627–637. [PubMed: 23948876]
8. Siminoski K, Lee KC, Jen H, et al. Anatomical distribution of vertebral fractures: comparison of pediatric and adult spines. Osteoporos Int. 2012; 23:1999–2008. [PubMed: 22109742]
9. Moore, KL.; Persaud, TVN. The skeletal system. The developing human: clinically oriented embryology. W.B. Saunders; Philadelphia, PA, USA: 1993. p. 354-369.
10. Resnick D, Niwayama G. Intravertebral disk herniations: cartilaginous (Schmorl's) nodes. Radiology. 1978; 126:57–65. [PubMed: 339268]
11. Bagnall KM, Harris PF, Jones PR. A radiographic study of the human fetal spine. 2. The sequence of development of ossification centres in the vertebral column. J Anat. 1977; 124:791–802. [PubMed: 604345]
12. Bick EM, Copel JW. Longitudinal growth of the human vertebra; a contribution to human osteogeny. J Bone Joint Surg Am. 1950; 32:803–814. [PubMed: 14784489]
13. Yu SW, Sether LA, Ho PS, et al. Tears of the anulus fibrosus: correlation between MR and pathologic findings in cadavers. AJNR Am J Neuroradiol. 1988; 9:367–370. [PubMed: 3128085]
14. Jones MD, Pais MJ, Omiya B. Bony overgrowths and abnormal calcifications about the spine. Radiol Clin North Am. 1988; 26:1213–1234. [PubMed: 3140288]
15. Cil A, Yazici M, Uzumcugil A, Kandemir U, Alanay A, Alanay Y, Acaroglu RE, Surat A. The evolution of sagittal segmental alignment of the spine during childhood. Spine. 2005; 30:93–100. [PubMed: 15626988]
16. Clowes, JA.; Eastell, R. Vertebral Fracture Assessment. In: Rosen, CJ., editor. Primer on the Metabolic Bone Diseases and Disorders of Mineral Metabolism. 7. American Society for Bone and Mineral Research; Washington DC: 2008. p. 186-193.
17. Lentle BC, Brown JP, Khan A, et al. Recognizing and reporting vertebral fractures: reducing the risk of future osteoporotic fractures. Can Assoc Radiol J. 2007; 58:27–36. [PubMed: 17408160]
18. Pandya NA, Meller ST, MacVicar DCR, et al. Vertebral compression fractures in acute lymphoblastic leukaemia and remodelling after treatment. Arch Dis Child. 2001; 85:492–493. [PubMed: 11719337]
19. Bjerregaard LL, Rosthooj S. Vertebral compression and eosinophilia in a child with acute lymphatic leukemia. J Pediatr Hematol Oncol. 2002; 24:313–315. [PubMed: 11972103]
20. Oliveri MB, Mautalen CA, Rodriguez Fuchs CA, Romanelli MC. Vertebral compression fractures at the onset of acute lymphoblastic leukemia in a child. Henry Ford Hosp Med J. 1991; 39:45–48. [PubMed: 1830297]
21. Carberry GA, Pooler BD, Binkley N, et al. Unreported vertebral body compression fractures at abdominal multidetector CT. Radiology. 2013; 268:120–126. [PubMed: 23449956]
22. Jiang G, Eastell R, Barrington NA, Ferrar L. Comparison of methods for the visual identification of prevalent vertebral fracture in osteoporosis. Osteoporos Int. 2004; 15:887–896. [PubMed: 15071725]

23. Genant HK, Wu CY, van Kuijk C, Nevitt MC. Vertebral fracture assessment using a semiquantitative technique. J Bone Miner Res. 1993; 8:1137–1148. [PubMed: 8237484]
24. Siminoski K, Lentle B, Matzinger MA, et al. Observer agreement in pediatric semiquantitative vertebral fracture diagnosis. Pediatr Radiol. 2014; 44:457–466. [PubMed: 24323185]
25. Giglio CA, Volpon JB. Development and evaluation of thoracic kyphosis and lumbar lordosis during growth. J Child Orthop. 2007; 1:187–193. [PubMed: 19308494]
26. Gaca AM, Barnhart HX, Bisset GS 3rd. Evaluation of wedging of lower thoracic and upper lumbar vertebral bodies in the pediatric population. AJR Am J Roentgenol. 2010; 194:516–520. [PubMed: 20093618]
27. Ferrar L, Jiang G, Armbrecht G, et al. Is short vertebral height always an osteoporotic fracture? The Osteoporosis and Ultrasound Study (OPUS). Bone. 2007; 41:5–12. [PubMed: 17499570]
28. Swischuk LE. The beaked, notched, or hooked vertebra: its significance in infants and young children. Radiology. 1970; 95:661–664. [PubMed: 4245629]
29. Levin TL, Berdon WE, Lachman RS, et al. Lumbar gibbus in storage diseases and bone dysplasias. Pediatr Radiol. 1997; 27:289–294. [PubMed: 9094231]
30. Dietz GW, Christensen EE. Normal “Cupid’s bow” contour of the lower lumbar vertebrae. Radiology. 1976; 121:577–579. [PubMed: 981649]
31. Tsuji H, Yoshioka T, Sainoh H. Developmental balloon disc of the lumbar spine in healthy subjects. Spine. 1985; 10:907–911. [PubMed: 2938273]
32. Chan KK, Sartoris DJ, Haghighi P, et al. Cupid’s bow contour of the vertebral body: evaluation of pathogenesis with bone densitometry and imaging-histopathologic correlation. Radiology. 1997; 202:253–256. [PubMed: 8988219]
33. Kyere KA, Than KD, Wang AC, et al. Schmorl’s nodes. Eur Spine J. 2012; 21:2115–2121. [PubMed: 22544358]
34. Tsirikos AI, Jain AK. Scheuermann’s kyphosis; current controversies. J Bone Joint Surg Br. 2011; 93:857–864. [PubMed: 21705553]
35. Lowe TG, Line BG. Evidence based medicine: analysis of Scheuermann kyphosis. Spine. 2007; 32:S115–119. [PubMed: 17728677]
36. McNaught, JM. PhD Thesis. Department of Archaeology. Durham University; Durham: 2006. A clinical and archaeological study of Schmorl’s Nodes: using clinical data to understand the past.
37. Madani G, Papadopoulou AM, Holloway B, et al. The radiological manifestations of sickle cell disease. Clin Radiol. 2007; 62:528–538. [PubMed: 17467389]
38. Chapelon E, Garabedian M, Brousse V, et al. Osteopenia and vitamin D deficiency in children with sickle cell disease. Eur J Haematol. 2009; 83:572–578. [PubMed: 19682065]
39. Hensinger RN. Spondylolysis and spondylolisthesis in children. Instr Course Lect. 1983; 32:132–151. [PubMed: 6546062]
40. Murase M. Clinical and radiological surveys of lumbar spondylolysis in young soccer players. Nihon Seikeigeka Gakkai zasshi. 1989; 63:1297–1305. [PubMed: 2614161]
41. Huang RP, Bohlman HH, Thompson GH, Poe-Kochert C. Predictive value of pelvic incidence in progression of spondylolisthesis. Spine. 2003; 28:2381–2385. [PubMed: 14560087]
42. Kumar R, Guinto FC Jr, Madewell JE, et al. The vertebral body: radiographic configurations in various congenital and acquired disorders. Radiographics. 1988; 8:455–485. [PubMed: 3380991]

The Canadian STeroid-associated Osteoporosis in the Pediatric Population (STOPP) Consortium (a pan-Canadian, pediatric bone health working group)

Co-ordinating Center

Children’s Hospital of Eastern Ontario, Ottawa, Ontario: Leanne M. Ward[#*§] (Study Principal Investigator), Janusz Feber[*§] (Nephrology), Jacqueline Halton[*§] (Oncology),

Roman Jurencak (Rheumatology), MaryAnn Matzinger (Radiology, Central Radiograph Analyses), Johannes Roth (Rheumatology), Nazih Shenouda[§] (Radiology, Central Radiograph Analyses), Jinhui Ma (Research Methods and Statistics)

Ottawa Hospital Research Institute, Ottawa Methods Centre Ottawa, Ontario: David Moher[*§] (Research Methods), Monica Taljaard (Research Methods and Statistics)

Participating Centers

Alberta Children's Hospital, Calgary, Alberta: Josephine Ho (Site Principal Investigator, from July 2013 to present), David Stephure (Bone Health, Site Principal investigator until July, 2013), Reinhard Kloiber (Radiology), Victor Lewis (Oncology), Julian Midgley (Nephrology), Paivi Miettunen (Rheumatology)

British Columbia Children's Hospital, Vancouver, British Columbia: David Cabral[*] (Site Principal Investigator), David B. Dix (Oncology), Kristin Houghton (Rheumatology), Helen R. Nadel (Radiology)

British Columbia Women's and Children's Hospital and Health Sciences Center, Vancouver, British Columbia: Brian C. Lentle[§] (Radiology)

Brock University, Faculty of Applied Health Sciences, St. Catharines, Ontario: John Hay[§] (Physical Activity Measurements)

Children's Hospital, London Health Sciences Centre, University of Western Ontario, London, Ontario: Robert Stein (Site Principal Investigator), Elizabeth Cairney (Oncology), Cheril Clarson (Bone Health), Guido Filler (Nephrology)[§], Joanne Grimmer (Nephrology), Scott McKillop (Radiology, from 2012 to present), Keith Sparrow (Radiology, until 2012)

IWK Health Center, Halifax, Nova Scotia: Elizabeth Cummings (Site Principal Investigator), Conrad Fernandez (Oncology), Adam M. Huber[§] (Rheumatology), Bianca Lang[*§] (Rheumatology), Kathy O'Brien (Radiology)

McMaster Children's Hospital, Hamilton, Ontario: Stephanie Atkinson[*§] (Site Principal Investigator), Steve Arora (Nephrology), Ronald Barr[§] (Oncology), Craig Coblentz (Radiology), Peter B. Dent (Rheumatology), Maggie Larche (Rheumatology)

Montréal Children's Hospital, Montréal, Québec: Anne Marie Sbrocchi (Site Principal Investigator, from 2013 to present), Celia Rodd[§] (Site Principal Investigator, until 2013), Sharon Abish (Oncology), Lorraine Bell (Nephrology), Claire LeBlanc (Rheumatology), Rosie Scuccimarri (Rheumatology)

Shriners Hospital for Children, Montréal, Québec: Frank Rauch[*§] (Co-Chair, Publications and Presentations Committee and Ancillary Studies Committee)

[#]Principal Investigator;
[*]Executive Committee Member;
[§]Publications and Presentations Committee Member

Ste. Justine Hospital, Montréal, Québec: Nathalie Alos[*] (Site Principal Investigator), Josée Dubois (Radiology), Caroline Laverdière (Oncology), Véronique Phan (Nephrology), Claire Saint-Cyr (Rheumatology)

Stollery Children's Hospital, Edmonton, Alberta: Robert Couch[*] (Site Principal Investigator), Janet Ellsworth (Rheumatology), Maury Pinsk (Nephrology), Jacob Jaremko and Kerry Siminoski[§] (Radiology), Beverly Wilson (Oncology),

Toronto Hospital for Sick Children, Toronto, Ontario: Ronald Grant[*] (Site Principal Investigator), Martin Charron (Radiology, until 2013), Diane Hebert (Nephrology)

Université de Sherbrooke, Department of family medicine, Sherbrooke, Québec: Isabelle Gaboury[*§] (Biostatistics)

Winnipeg Children's Hospital, Winnipeg, Manitoba: Shayne Taback[§] (Site Principal Investigator), Tom Blydt-Hansen (Nephrology), Sara Israels (Oncology), Kiem Oen (Rheumatology), Martin Reed (Radiology), Celia Rodd[§] (Bone Health, from 2013 to present)

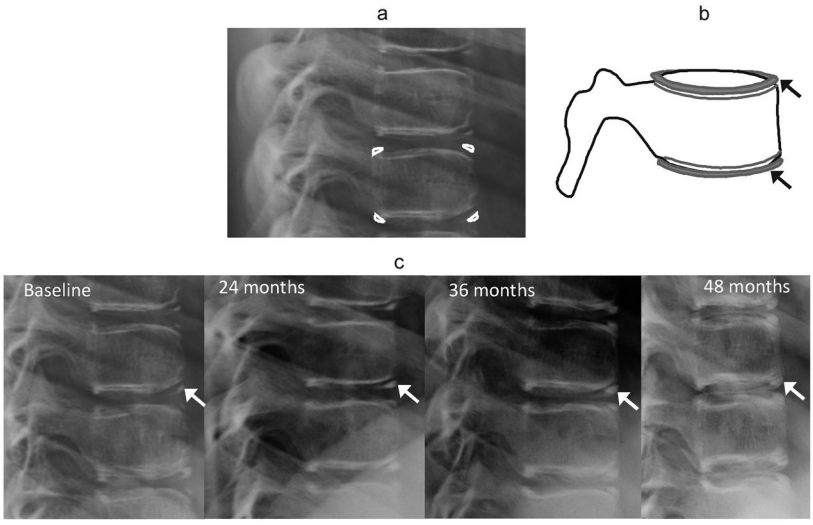

Fig. 1.

Ring apophyses. (a) Lateral radiograph ossification of ring apophyses in a 10 year-old girl on glucocorticoid treatment for chronic renal disease. (b) Corresponding diagram of development of ring apophyses at endplate margins *(arrows*). (c) Lateral radioography shows ossification and fusion of ring apophyses (*arrows*) over a four year period in the same girl

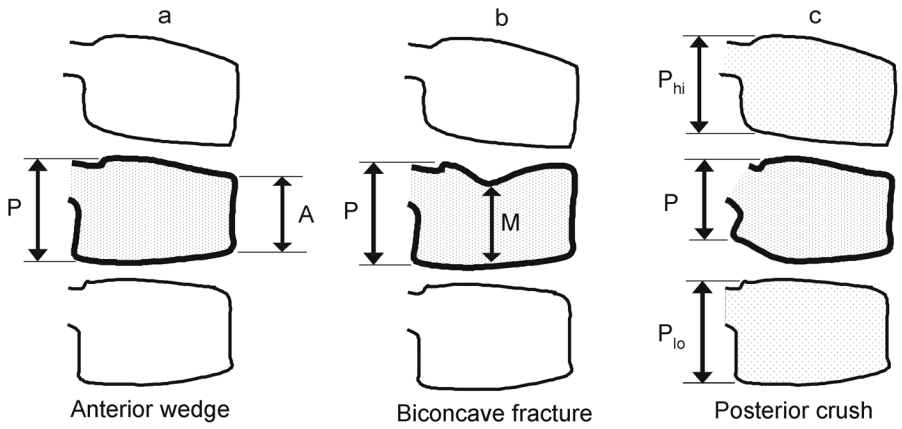

Fig. 2.

Diagram of the Genant semi-quantitative grading system for vertebral compression fractures. (a) Anterior wedging: measure the anterior height loss relative to posterior height (i.e., ratio = (P−A)/P × 100%). (b) Biconcave fracture: measure the minimum central vertebral body height relative to posterior height (i.e., ratio = (P−M)/P × 100%). Note that this fracture description is a misnomer because in many cases only one endplate is involved; the term is retained for fidelity with the original Genant grading system. (c) Posterior crush: because the posterior body wall is altered in this type of fracture and cannot serve as its own reference, this height should be measured relative to the posterior height of the adjacent vertebrae. The lower of the two ratios (Phi–P)/Phi and (Plo–P)/Plo is recorded as a percentage. Because L4 is the lowest level scored in Genant, at L4 only the L3 posterior height is used for comparison. Genant grades are: 0, height loss 20% or less; 1 (mild), >20–25%; 2 (moderate), >25–40%; 3 (severe), >40%. (Conceptually similar to figures in Genant 1993, [23], and Siminoski 2014, [24])

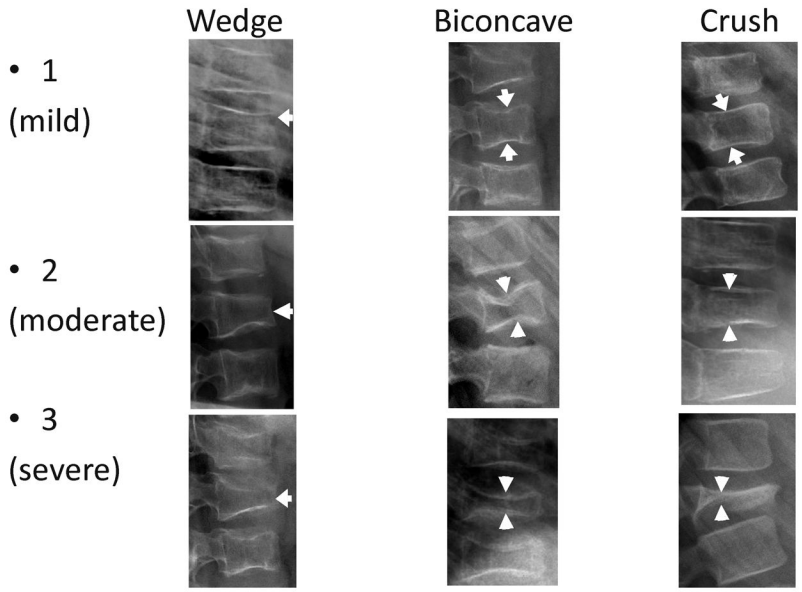

Fig. 3.

Examples of actual fractures of each subtype in the Genant semi-quantitative grading system. All images are sagittal radiographs of thoracolumbar vertebrae oriented with anterior to the right. Top row: 5 year-old girl with acute lymphoblastic leukemia; 9 year-old girl with acute lymphoblastic leukemia; 6 year-old boy with acute lymphoblastic leukemia. Middle row: 10 year-old girl with acute lymphoblastic leukemia; 10 year-old girl with osteogenesis imperfecta; 5 year-old girl with acute lymphoblastic leukemia. Bottom row: 9 year-old girl with acute lymphoblastic leukemia; 8 year-old girl with acute lymphoblastic leukemia; 10 year-old boy with histiocytosis. *Arrows* indicate the fracture in each image. In the image of grade 2 crush fracture, note also the grade 1 wedge fracture at the vertebra below

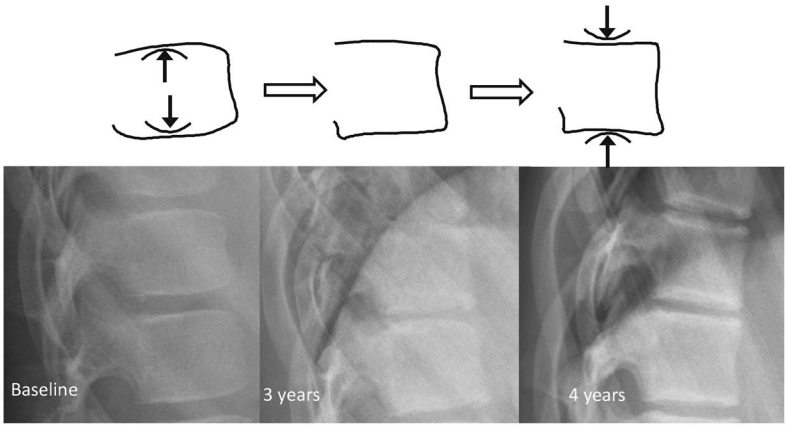

Fig. 4.

Normal progression from convex to concave endplates at T12 and L1 over 4 years, in a girl on glucocorticoid treatment for nephrotic syndrome, first imaged at age 9 years. Note also the ossification and fusion of ring apophyses during this time, which contributes to the final apparent concavity of endplates, as seen on lateral radiography.

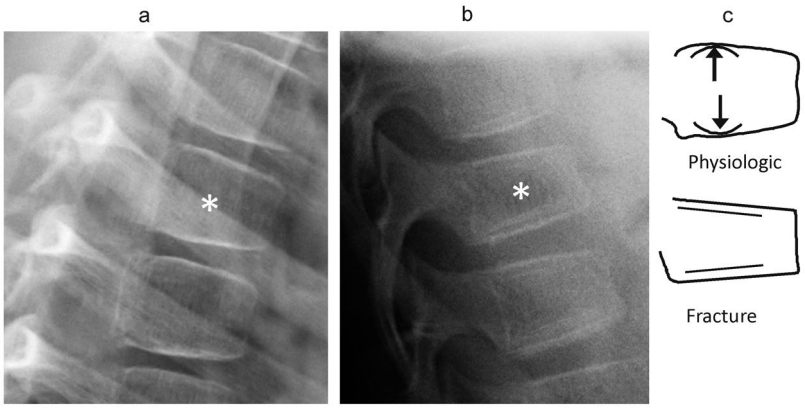

Fig. 5.

(a) Anterior lateral radiographs shows exaggerated anterior wedging (near 25% height loss) in a mid-thoracic vertebra (*), in a 7 year-old girl treated with glucocorticoids for linear scleroderma. This was present and unchanged on all scans for 3 years. (b) Lateral radiograph shows a wedge compression fracture with near 25% anterior height loss at T11 (*), in a 9 year-old girl treated with glucocorticoids for acute lymphoblastic leukemia. (c) Diagram distinguishes between these. In both cases the endplates appear uninterrupted such that this criterion is not helpful. Note that in the upper schematic vertebra, drawn from image (a), the posterior portions of the endplates retain their normal childhood convexity, while in the lower vertebra, drawn from image (b), the endplates are flattened and linear. Also, (b) shows a double endplate contour (bone-in-bone), which, although nonspecific, can be seen during fracture healing

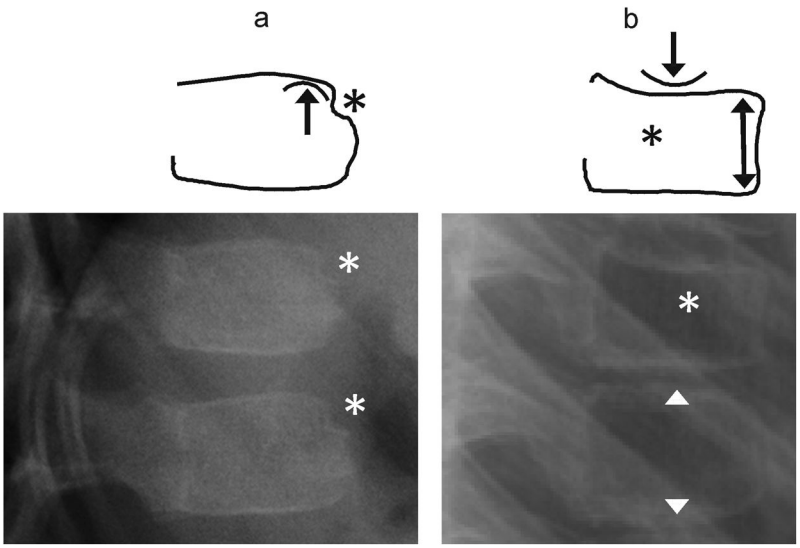

Fig. 6.

Indentation at an anterior ring apophysis vs. fracture. (a) Step deformities (*) at anterior superior endplates of T12 and L1 in a 5 year-old boy treated with glucocorticoids for nephrotic syndrome represent prominent notches at the as yet un-ossified anterior ring apophysis. A clue that this is a normal variant is the preserved outward convexity of the endplates immediately posterior to this. The anterior cortex should be stronger than the trabecular bone just posterior to it, so a fracture involving anterior cortex ought to also depress the endplate posterior to it. (b) Typical lateral radiographic appearance of a thoracic compression fracture (*), in a 10 year-old boy treated with glucocorticoids for acute lymphoblastic leukemia. Although there is some anterior height loss, the greatest height loss is in the mid-vertebra, where little vertically oriented cortical bone is available to protect from compressive loading. The endplate is concave upward just posterior to the anterior cortex, rather than convex as in image (a). Note the normal convex-outward appearance of the lower vertebra seen in image (b) (*arrowheads*)

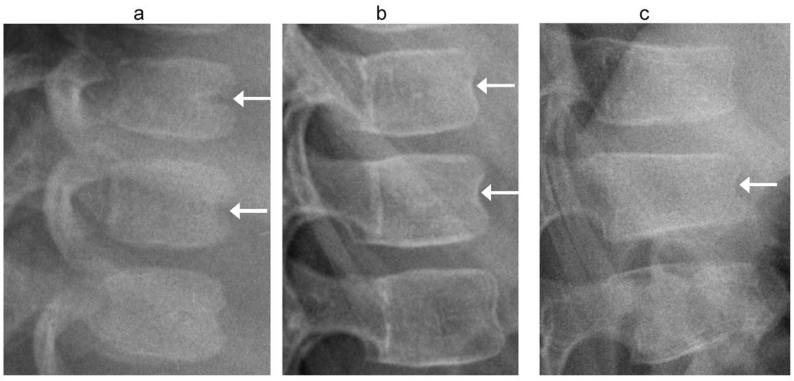

Fig. 7.

Anterior vertebral wall vascular groove vs. fracture. (a) Lateral radiograph shows a typical linear indentation *(arrows)* at mid-anterior vertebral body wall representing a vertebral artery groove, in a 1.4 year-old girl treated with glucocorticoids for juvenile inflammatory arthritis. This is unlikely to be confused with fracture. (b) Lateral radiograph shows residual indentation *(arrows)* at anterior vertebral body walls from ossifying vertebral artery grooves in a 5 year-old girl, with. (c) In this anterior wedge compression fracture *(arrow)* in a 7 year-old boy with linear flattening of endplates, the indentation of anterior cortex is similar to image (b) and may be incidental. The children in (b) and (c) were both treated with glucocorticoids for acute lymphoblastic leukemia

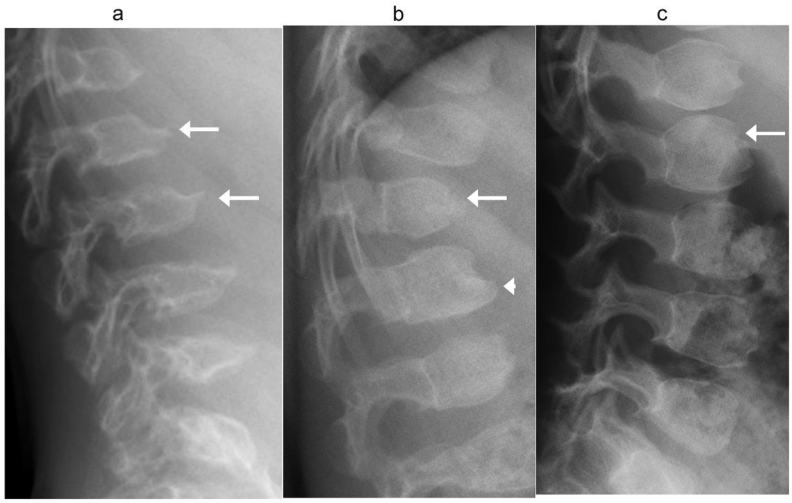

Fig. 8.

Anterior vertebral beaking at upper lumbar vertebrae in mucopolysaccharidoses, for comparison with normal variation. (a) Lateral radiograph in a 5 year-old boy with Morquio syndrome shows typical central beaking most pronounced at L1 and L2 *(arrows)*. (b) Lateral radiograph in a 4 year-old boy with Hurler syndrome shows hypoplastic anterior aspect of T12 with gibbus deformity *(arrow)*, and inferior beaking at L1 *(arrowhead)*. (c) Lateral radiograph in a 4 year-old boy with Hunter syndrome shows exaggerated convexity of vertebral body contours, which appear rounded, with prominent impressions at un-ossified ring apophyses *(arrow)*

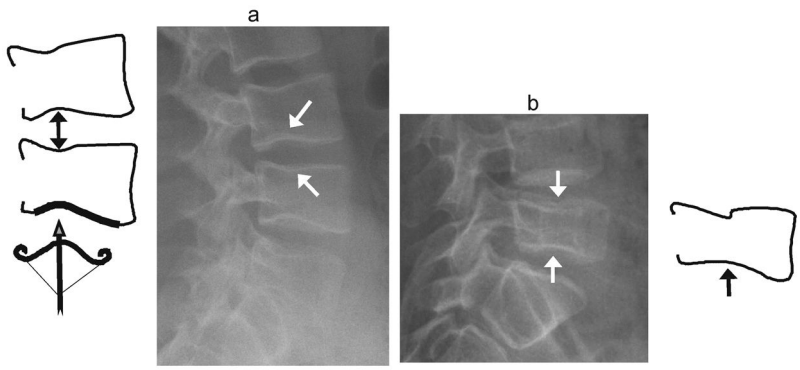

Fig. 9.

Cupid's bow vs. biconcave fracture. (a) Diagram and lateral radiograph depict Cupid's bow or balloon disk at multiple levels in a 17 year-old boy treated with glucocorticoids for vasculitis. This normal variant is a curved indentation centred at the posterior third of the endplate *(arrows).* The shape resembles Cupid's bow (diagram, bottom), and when present at adjacent endplates, it gives the impression of disk expansion, hence it is also known as 'balloon disk'. (b) Biconcave endplate fracture at L5, in a 10 year-old boy treated with glucocorticoids for acute lymphoblastic leukemia. There is interruption of the superior endplate of L5, the endplate concavities are centered at the mid-disk rather than the posterior third, there is overall height loss, and adjacent levels are not affected

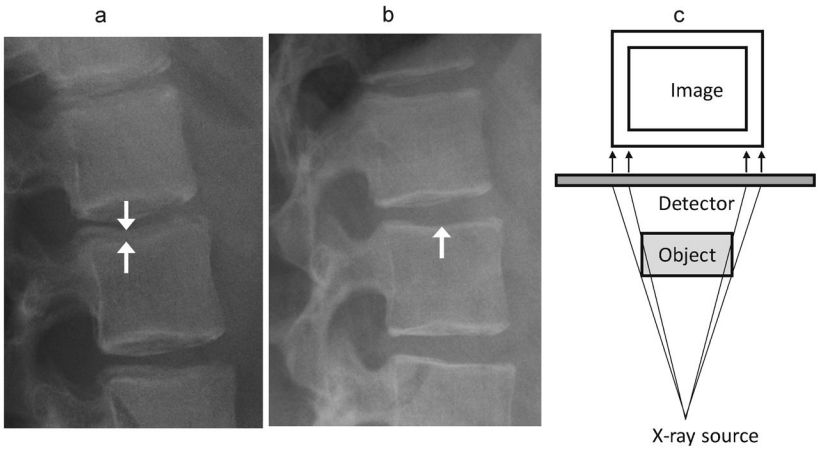

Fig. 10.

Parallax effect. (a) Lateral radiographs of the upper lumbar spine in a 12 year-old girl treated with glucocorticoids for mixed connective tissue disease shows non-overlapping endplates, especially at L2 (*arrows*), due to parallax. (b) A follow-up image obtained 3 years later shows overlapping endplates without parallax effect (*arrow*). (c) Diagram of parallax effect. The side of the object closest to the X-ray source is magnified and eccentrically positioned compared to the other side. For vertebrae, this gives an appearance of bone-in-bone, or endplate interruption. This is minimized by using a source as far away as possible, and centering the beam appropriately

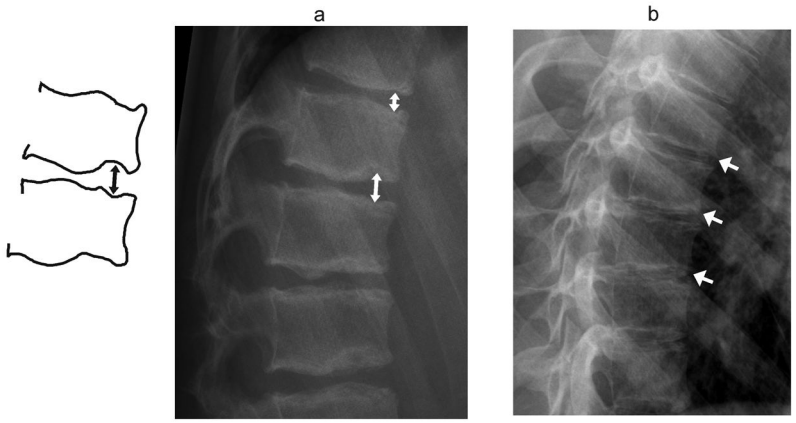

Fig. 11.

Normal variants involving irregular endplates. (a) Diagram and lateral radiograph shows multiple Schmorl nodes near thoracolumbar junction *(arrows)* in a 16 year-old boy treated with glucocorticoids for vasculitis. The endplates are irregular with areas of focal depression and sclerosis implying sites of intraosseous disk herniation. There is only minimal anterior wedging, not meeting criteria for wedge compression fracture. (b) Lateral radiograph shows Scheuermann kyphosis in a 14 year-old girl treated with glucocorticoids for dermatomyositis. Endplate irregularity and mild anterior wedging are seen at multiple mid-thoracic levels, resulting in increased kyphosis

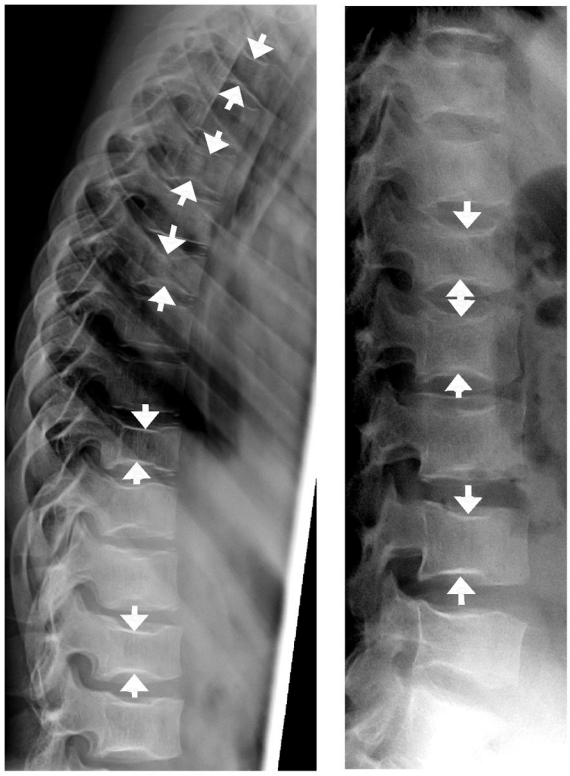

Fig. 12.

Sickle cell anemia. Lateral radiographs (a, b) show central endplate deformity at multiple levels in 13 year-old girl with sickle cell anemia, mimicking biconcave endplate compression fractures. Nearly all levels are involved to variable extent, with *arrows* showing some of the most prominent endplate depressions in this girl

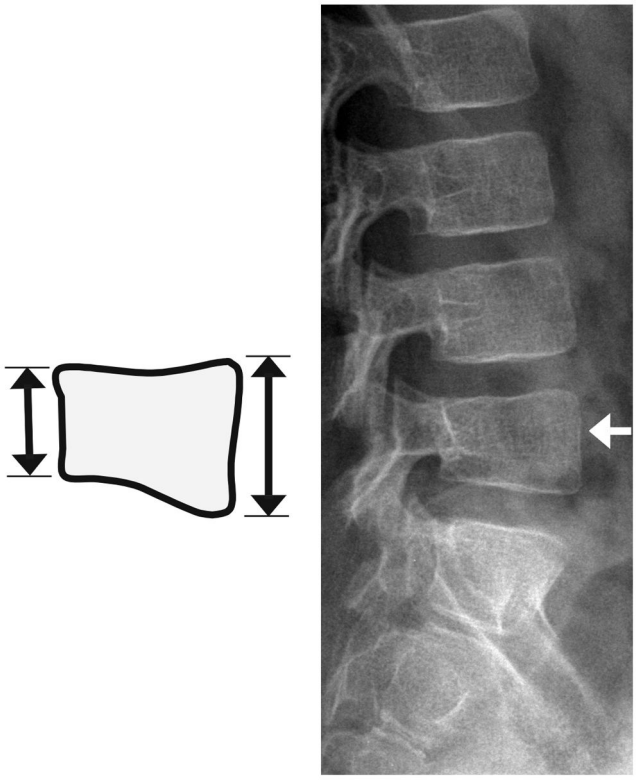

Fig. 13.

Trapezoidal L5. Diagram and lateral radiograph shows a shorter posterior wall than anterior of L5 *(arrow)*, giving a trapezoidal vertebral body shape in a 7- year-old girl with mixed connective tissue disease. This does not represent a posterior crush fracture, but is a normal variation

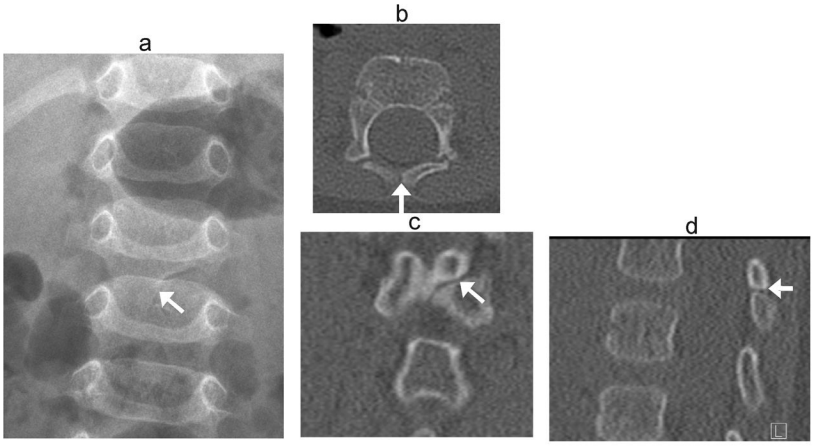

Fig. 14.

Incomplete midline fusion. Developmental cleft mimics fracture in a 6 –month- old boy transferred to tertiary hospital after fall from bed. Radiographs were reported as showing a vertebral fracture. (a) Anteroposterior radiograph shows oblique lucency at posterior elements of L2 *(arrow).* (b) Axial, (c) coronal and (d) sagittal CT images in bone windows demonstrate smooth, sclerotic margins at the oblique developmental cleft *(arrows)*

TABLE 1

Summary of Common Normal Variants Mimicking Fractures in the Pediatric Thoracolumbar Spine

Location	Variant	Features
Anterior	Physiologic wedging	Thoracolumbar junction, <11% height loss, outward convexity of endplates may be preserved (Fig. 5)
	Ring apophyses	Notch at anterior vertebral wall, preserved endplate convexity nearby (Fig. 6)
	Vertebral artery impression	Thin and linear, multiple levels (Fig. 7)
	Anterior beaking	Near thoracolumbar junction, central or inferior beaking, associated with neuromuscular disease or skeletal dysplasias; often involves multiple levels (Fig. 8)
Central	Cupid's bow or balloon disk	Undulating depression of posterior third of endplate, usually at both sides of disc space at lower lumbar levels (Fig. 9)
	Parallax artifact	Non-overlapping endplates, progressively worsens toward edges of film (Fig. 10)
	Schmorl node	Lower thoracic to upper lumbar spine, focal depression of endplate, remainder of endplate is intact, lack of overall height loss. (Fig. 11)
	Scheuermann's disease	At least 3 adjacent levels with mild anterior wedging and irregular endplates, thoracic kyphosis >45° (Fig. 11)
Posterior	Trapezoidal L5	Taller L5 anterior vertebral body than posterior; may have flattened lumbar lordosis and relatively horizontal sacrum; often associated with spondylolysis (Fig. 13)
	Incomplete midline fusion	Fissure may mimic fracture if obliquely oriented (Fig. 14)